Experimental Determination of Solid-Liquid-Liquid Equilibrium Phase Diagrams

Sau M. Lai, Mai Y. Yuen, Leo K. S. Siu, and Ka M. Ng
Dept. of Chemical Engineering, The Hong Kong University of Science and Technology, Clear Water Bay, Hong Kong

Christianto Wibowo
ClearWaterBay Technology, Inc., 4000 W. Valley Blvd., Suite 100, Pomona, CA 91789

DOI 10.1002/aic.11183
Published online April 20, 2007 in Wiley InterScience (www.interscience.wiley.com).

Liquid–liquid phase separation is undesirable in crystallization as it leads to slow crystal growth and uncontrollable crystal morphology. Therefore, it is necessary to identify the conditions under which liquid–liquid phase split occurs, so as to avoid crystallization process taking place at such conditions. In this study, an experimental approach is developed to systematically construct the solid-liquid-liquid equilibrium (SLLE) phase diagram. A four-component system is used to demonstrate the experimental technique and the overall workflow in developing an SLLE phase diagram.
 AIChE J, 53: 1608–1619, 2007
Keywords: phase diagrams, solid-liquid-liquid equilibrium, crystallization, oiling out, process synthesis

Introduction

Crystallization is commonly used in chemical processes for the production of solids, such as the manufacture of inorganic salts, detergents, fertilizers, insecticides, herbicides, and pharmaceuticals. When components of different polarities are involved, undesirable liquid–liquid phase split may occur during the course of crystallization.[1] This so-called oiling out phenomenon is often accompanied by the formation of liquid droplets on the crystal surface, leading to slow crystal growth, uncontrollable crystal morphology, and crystal inhomogeneity. Another common symptom is the formation of a dumpling-like substance consisting of agglomerated solid particles within one of the immiscible liquid phases. Oiling out during crystallization has been observed in a variety of systems, including lysozyme (in water),[2] bisphenol A (in water),[3] drug substance $C_{35}H_{41}Cl_2N_3O_2$ (in water/ethanol mixture),[4,5] and poly(ethylene-*co*-vinyl alcohol) (in glycerol).[6] Processes involving oiling out are often deemed not scalable because of the difficulty in controlling the crystal quality.

To ensure a trouble-free process, liquid–liquid phase split during crystallization must be avoided.[7] Therefore, it is important to identify the conditions, including feed composition and crystallization temperature, under which liquid–liquid phase split occurs. A solid-liquid-liquid equilibrium (SLLE) phase diagram can be constructed to represent the phase behavior of the system, showing the different regions where single or multiple phases coexist. With the SLLE phase diagram in place, the crystallizer operating condition can be chosen to avoid getting into the liquid–liquid phase split region. For this purpose, an efficient method to determine SLLE phase diagrams is highly desirable.

Experimental techniques to obtain phase diagrams have been reported in the literature. For example, visualization method based on the disappearance of solid phase has been suggested to determine solid–liquid equilibrium (SLE) phase diagrams which do not involve liquid–liquid phase split.[8] Investigation of liquid–liquid equilibrium (LLE) behavior

Correspondence concerning this article should be addressed to K. M. Ng at kekmng@ust.hk.

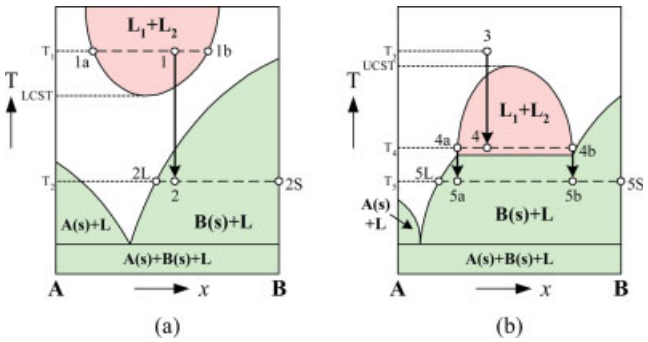

Figure 1. Polythermal SLLE phase diagram of a binary system: (a) with an LCST and no intersection between LLE and SLE regions; (b) with a UCST and intersecting LLE and SLE regions.

[Color figure can be viewed in the online issue, which is available at www.interscience.wiley.com.]

normally involves analytical methods to determine the tie lines in the liquid–liquid phase split region.[9] This method is often tedious and time-consuming. For the purpose of preventing oiling out, however, only the boundaries of the liquid–liquid phase split region are of interest and it is not essential to determine the tie lines. With this in mind, this article proposes a novel experimental strategy to quickly identify the liquid–liquid phase split region as well as the SLE boundaries in an SLLE phase diagram.

Phase Behavior

Before proceeding to the details of the strategy, an overview of the key features of SLLE phase behavior of systems involving two, three, and four components is given below.

Binary system

Figure 1 shows phase diagrams featuring two different types of isobaric SLLE phase behavior of a binary system, with various regions where multiple phases coexist in equilibrium marked on the diagrams. Such diagrams are generally referred to as polythermal diagrams, as they demonstrate the phase behavior at multiple temperatures. A simple eutectic behavior is assumed between components A and B.

In Figure 1a, the LLE region features a lower critical solution temperature (LCST) and does not intersect with any of the SLE regions. At temperature T_1, a mixture with an overall composition represented by point 1 lies inside the LLE region, thereby splitting into two phases. The equilibrium compositions of the two separate liquid phases (shown as points 1a and 1b) are governed by the tie-line. However, cooling of this mixture below the LCST would lead to the formation of a single liquid phase, which would separate into solid B (point 2S) and a liquid phase (point 2L) when cooled down further to temperature T_2. Therefore, liquid–liquid phase split and crystallization do not occur simultaneously, and oiling out will never be observed. In this case, it is sufficient to locate only the SLE region for designing the crystallization process.

Figure 1b depicts another type of SLLE phase behavior, featuring an LLE region with an upper critical solution temperature (UCST) intersecting with the SLE region. When a mixture with composition shown as point 3 is cooled down to temperature T_4, liquid–liquid phase split takes place, resulting in a heterogeneous mixture of two liquid phases with different compositions (points 4a and 4b). When the temperature is further reduced to temperature T_5, solid B would crystallize out to give a liquid of composition of point 5L. However, crystallization from point 4a occurs with a lower degree of supersaturation compared to that from point 4b. Droplets or blobs of one phase would interfere with crystallization in the continuous phase, forming dumpling-like crystals of unacceptable quality.

Ternary system

The isobaric (polythermal) SLLE phase diagram for a ternary system takes up the shape of a triangular prism, with a binary system phase diagram on each of its three rectangular faces. Figure 2a shows an example of such diagram involving components A, B, and S, in which A-B and B-S pairs exhibit the SLLE behavior depicted in Figure 1b (featuring a UCST and intersection between SLE and LLE regions). There is no liquid–liquid phase split observed between A and S. For easier examination of the various regions at different temperatures, isothermal cuts such as those shown in Figures 2b–d can be taken. Isothermal cuts are particularly suitable for displaying tie-lines showing the composition of phases that are in equilibrium with each other, because those phases must have the same temperature.

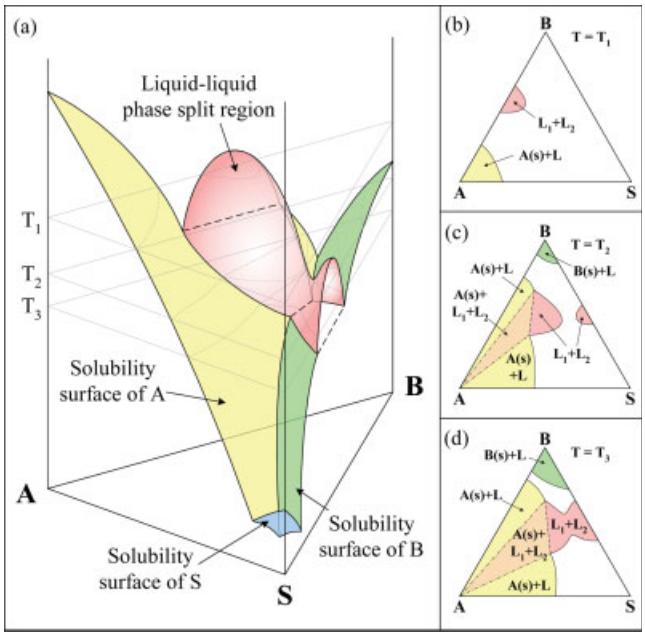

Figure 2. SLLE phase diagram of a ternary system: (a) polythermal phase diagram; (b) isothermal cut at T_1; (c) isothermal cut at T_2; (d) isothermal cut at T_3.

[Color figure can be viewed in the online issue, which is available at www.interscience.wiley.com.]

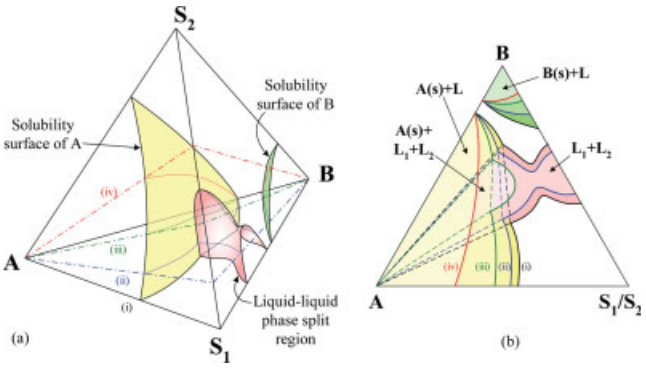

Figure 3. SLLE phase diagram of a quaternary system: (a) isothermal cut; (b) constant S_1:S_2 ratio cuts of the isothermal cut.

[Color figure can be viewed in the online issue, which is available at www.interscience.wiley.com.]

At temperature T_1 above the melting point of B, the isothermal cut (Figure 2b) features only one SLE region, inside of which solid A would crystallize out. There is also an LLE region extending from the A-B side, which is part of the three-dimensional liquid–liquid phase-split region shown in Figure 2a. Another cut taken at a lower temperature T_2 (Figure 2c) shows that the LLE region interferes with A(s)+L region, effectively dividing that region into two separate parts and creating a three-phase region inside of which solid A is in equilibrium with two liquid phases. There is also another LLE region emanating from the B-S edge, which is actually a part of the same three-dimensional liquid–liquid phase-split region of Figure 2a. Since T_2 is below the melting point of B, an SLE region where B would crystallize out also appears on the cut. As the temperature is further lowered to T_3 (Figure 2d), the two LLE regions merge to form a dumbbell-shaped region.

Quaternary system

A common example of a quaternary system is one that has two solutes and two solvents, for which the isobaric phase diagram has a dimensionality of four. Because of the high dimensionality, it is impossible to visualize the phase diagram in its entirety. To analyze the phase behavior of such a system, appropriate cuts and projections should be taken to reduce the dimensionality.[10] One option is to combine two components as a single pseudo-component, which produces a three-dimensional, polythermal constant-composition cut. Such a cut would look similar to Figure 2a. Isothermal cuts can then be taken to produce diagrams similar to Figures 2b–d. The major difference is that on these figures, most tielines cannot be displayed because their two ends do not actually lie on the same cut.

Figure 3 offers another perspective on the SLLE phase diagram of a quaternary system. Instead of taking a constant-composition cut, the original four-dimensional diagram can be represented by a series of isothermal cuts, one of which is shown in Figure 3a. The base of the tetrahedron (i) represents subsystem A-B-S_1, which corresponds to the triangle shown in Figure 2d. Three cuts at different S_1 to S_2 ratios (ii, iii, and iv) are shown in the figure. Expectedly, the cuts at different ratios feature different types and sizes of regions, as drawn in Figure 3b. Compared to cut (i), the liquid-liquid region in cut (ii) is smaller. This region shrinks further so that it no longer touches the B-S_1/S_2 edge in cut (iii), and disappears altogether in cut (iv). Consequently, the three-phase region A(s)+L_1+L_2 also disappears in cut (iv). Such behavior is possible when S_2 is miscible with S_1, so that the liquid mixture tends to become homogeneous as more S_2 is added to the system. Note that cuts (ii)–(iv) can also be obtained from the constant composition cuts at corresponding values of S_1 to S_2 ratio by taking an isothermal cut. Visualizing the phase behavior using a series of such isothermal cuts is often easier compared to having to analyze the 3D diagram.

Experimental Determination

As previously mentioned, with the objective of preventing oiling out during crystallization, only the boundaries of the liquid–liquid phase split region have to be identified. Then, the feed composition and crystallization temperature can be judiciously selected to avoid the liquid–liquid phase split region. To serve this purpose, an experimental strategy based on visual observation is proposed.

Known amounts of the desired components are first weighed into a jacketed glass vessel (Figure 4a). The mixture inside the vessel can be heated up or cooled down in a controlled manner by passing a heat transfer fluid through the glass jacket. The temperature of the mixture is measured

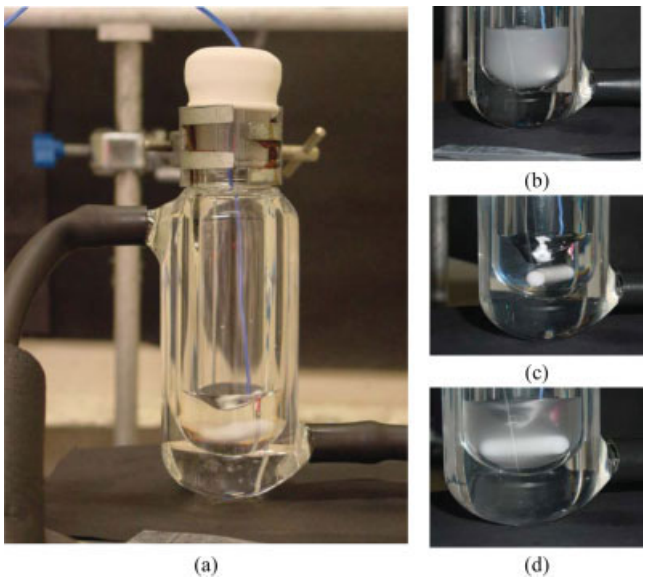

Figure 4. Determination of SLLE phase behavior using visual method: (a) experimental setup; (b) Heterogeneous mixture formed within a phase split region; (c) Homogeneous liquid formed upon heating above the disappearance temperature; (d) Heterogeneous mixture formed again upon cooling below the reappearance temperature.

[Color figure can be viewed in the online issue, which is available at www.interscience.wiley.com.]

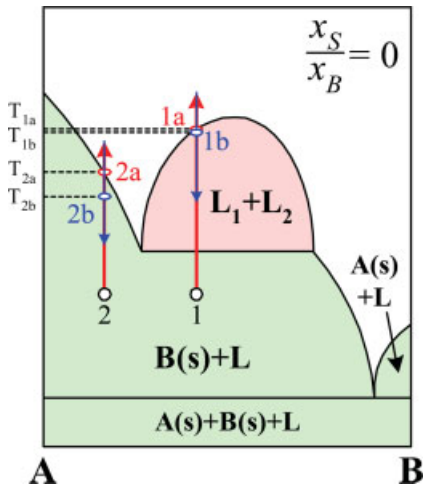

Figure 5. Experimental strategy for the determination of phase boundaries.

[Color figure can be viewed in the online issue, which is available at www.interscience.wiley.com.]

using a thermocouple. During the entire process, the mixture is continuously mixed by using a magnetic stirrer. The starting temperature is chosen such that the mixture is heterogeneous, as indicated by a turbid appearance (Figure 4b). The mixture is then heated up slowly until it forms a clear homogeneous solution (Figure 4c). The temperature at which the mixture becomes clear is recorded. Then, it is slowly cooled until the mixture again becomes cloudy (Figure 4d), indicating the appearance of a second phase. The temperature at which this new phase appears is also recorded. The experiment is then repeated with different mixture compositions so as to span the entire composition region of interest.

Although the disappearance and reappearance of a second phase can be visually observed, it is impossible to tell whether the second phase is liquid or solid, so that one cannot readily differentiate between a solid–liquid boundary and a liquid–liquid boundary. Fortunately, these can be distinguished by comparing the recorded disappearance and reappearance temperatures. As the rate of formation of liquid droplets is faster than that of crystal nuclei,[11] the formation of a second liquid phase happens soon after the mixture enters the LLE region, while nucleation occurs only after the mixture is subcooled 5–10°C below the thermodynamic dissolution temperature. Therefore, an LLE boundary is characterized by a small difference between the disappearance and reappearance temperatures, whereas for an SLE boundary the difference is much larger. This is illustrated in Figure 5. When a mixture with a composition indicated by point 1 is heated up, the solution becomes clear at the dissolution temperature T_{1a}, and turns cloudy at temperature T_{1b} when cooled back down. The small difference between these two temperatures indicates an LLE boundary. Meanwhile, heating of a mixture with another composition (point 2) results in complete dissolution at T_{2a}, and upon subsequent cooling the second phase reappears at T_{2b}. The relatively large difference between T_{2a} and T_{2b} indicates an SLE boundary.

Since each heating/cooling experiment described above only produces one point on either an SLE or LLE boundary, it has to be repeated for different compositions to span the

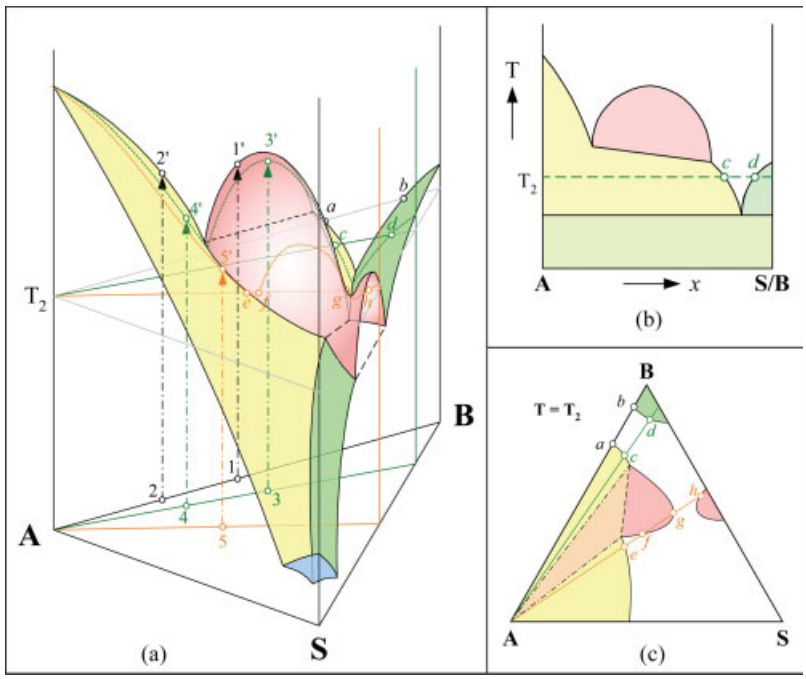

Figure 6. Data collection strategy for a ternary system: (a) Polythermal phase diagram with cuts at constant S:B ratios; (b) One of the cuts at a constant S:B ratio; (c) An isothermal cut at T_2 can be reconstructed from constant S:B ratio cuts.

[Color figure can be viewed in the online issue, which is available at www.interscience.wiley.com.]

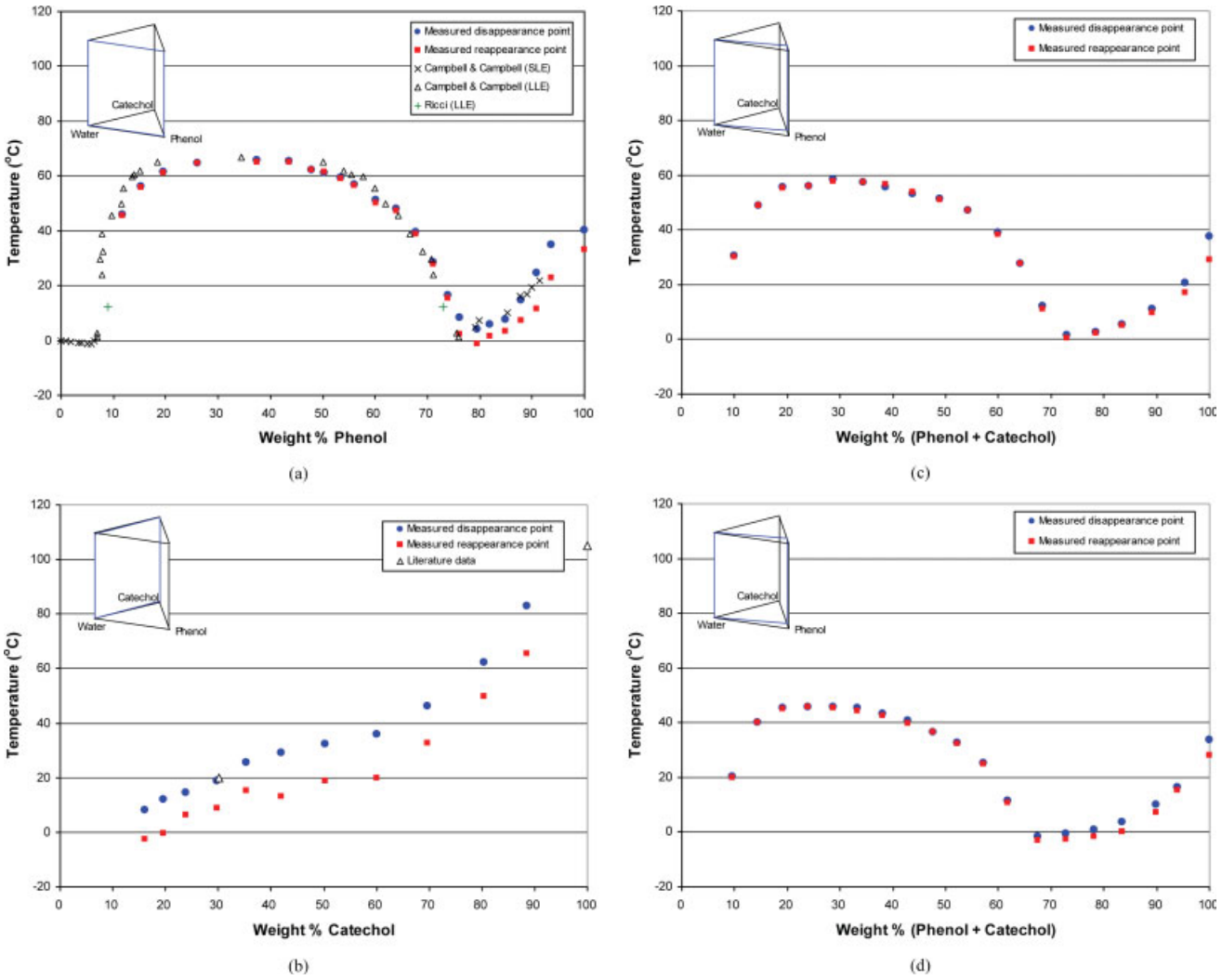

Figure 7. Experimental disappearance and reappearance temperatures for phenol/catechol/water systems: (a) phenol:catechol = 100:0, (b) phenol:catechol = 0:100, (c) phenol:catechol = 95:5, (d) phenol:catechol = 90:10, (e) phenol:catechol = 80:20, (f) phenol:catechol = 50:50, (g) phenol:catechol = 20:80.

[Color figure can be viewed in the online issue, which is available at www.interscience.wiley.com.]

entire composition space of interest. Figure 6 illustrates our strategy for data collection, using a ternary system as an example. First, a series of vertical cuts are arbitrarily chosen to form pseudobinary systems. For example, cuts at constant ratio of S to B can be taken, as shown in Figure 6a. To determine the phase boundaries at S:B = 0:100 (the back face of the prism), mixtures of A and B at different compositions (such as points 1 and 2) are prepared and their dissolution points (represented by points $1'$ and $2'$, respectively) are measured. The phase boundaries for other cuts at different values of S to B ratio (two of which are shown in Figure 6a) can be similarly determined.

For crystallization process design purposes, isothermal cuts are often more useful compared to constant ratio cuts generated using the above-mentioned method. By putting together a number of constant ratio cuts, the isothermal cuts can be readily obtained. Figure 6b shows one of the constant ratio cuts of the ternary phase diagram in Figure 6a. A horizontal line at a temperature of interest T_2 intersects the SLE boundaries at points *c* and *d*, which would appear at the isothermal cut at T_2. Similarly, other intersection points such as *a*, *b*, *e*, *f*, *g*, and *h* can be identified from cuts at other S to B ratios. These points define the phase boundaries on the isothermal cut at T_2 (Figure 6c). Isothermal cuts at other temperatures can also be obtained in the same way, that is, by locating the intersection points at the corresponding temperature.

Example

To demonstrate how the experimental technique and strategy described above can be applied in the determination of an SLLE phase diagram, a quaternary system containing catechol, phenol, water, and acetone is used as an example. Catechol is a dihydroxybenzene used as food, pharmaceutical, or agrochemical ingredients, with a global comsumption of about 20,000 tonnes per year in 1990.[12] It is typically pro-

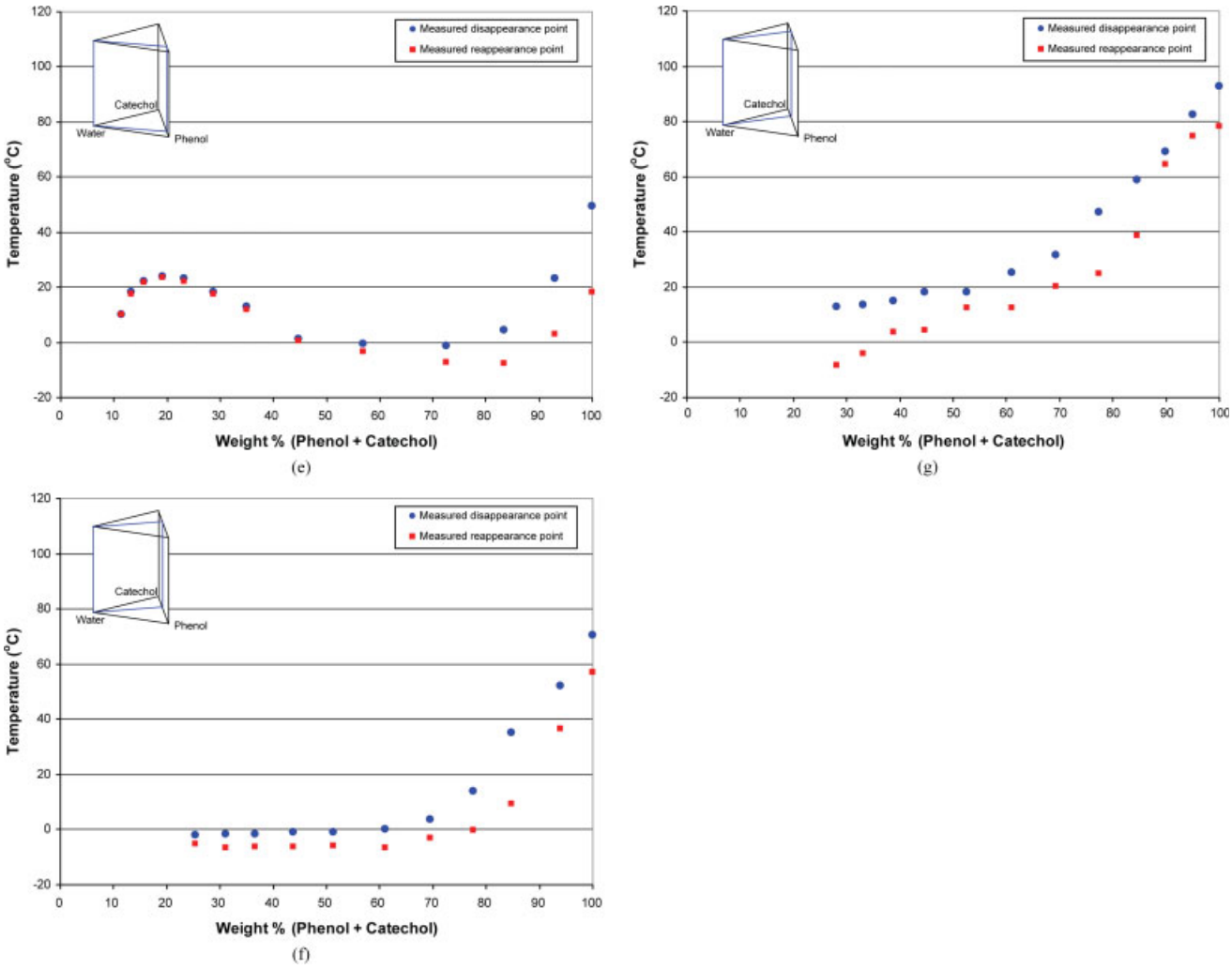

Figure 7. (*Continued*)

duced via catalytic hydroxylation of phenol, after which a stream containing catechol, unreacted phenol, and some impurities is produced. One process alternative to obtain pure catechol consists of a series of distillation columns to fractionate this reaction mixture.[13] Another alternative is to use distillation to remove high boiling impurities such as hydroquinone, followed by crystallization to obtain solid catechol product with high purity. This alternative is more attractive because of lower energy consumption.

Crystallization of catechol may be facilitated by the presence of an appropriate solvent. Water is a natural choice for crystallization solvent since it is often used as the medium for the hydroxylation reaction.[14] However, pure water may not be a desirable choice because of its relatively high latent heat of vaporization, which will lead to a large energy requirement for the solvent recovery system. The use of an organic solvent such as acetone may lower the burden on solvent recovery, but its high dissolving power may lead to a lower per-pass yield in the crystallizer. Therefore, a mixture of water and acetone seems to be a suitable solvent candidate. Because of the different polarity of the components in the system, it is important to take into account the possibility of liquid–liquid phase split. In fact, the presence of an LLE region has been reported in the literature for phenol/water binary system.[11,15] Therefore, an SLLE phase diagram is needed to design the crystallization process.

Polythermal plots

First of all, the ternary system phenol/catechol/water is analyzed. Figure 7 shows the experimental results (in weight percent basis) plotted on the polythermal phase diagram for this system. The results for phenol/water binary system are plotted in Figure 7a along with literature data. It can be seen that experimental data on the phenol-rich side (80 wt % phenol and above) expose a difference of 5–10°C between the disappearance and reappearance temperatures. This is a clear indication of an SLE boundary, which is supported by the fact that the measured dissolution temperatures are consistent with literature data from Campbell and Campbell.[15] On the other hand, the rest of the experimental data (between 12 wt % and 74 wt % phenol) show that within this composition range, the disappearance and reappearance temperatures are practically the same, indicating an LLE boundary. Again, these results are consistent with the reported LLE data in the literature.[11,15] Such a general agreement with literature data

Table 1. Summary of Experimental Results for Solvents Other Than Pure Water

Solvent Composition (Water:Acetone)	Solute Ratio (Phenol:Catechol)	Experimental Data			
		Weight % Solute	Disappearance Temperature (°C)	Reappearance Temperature (°C)	Indication*
75:25	100:0 (pure phenol)	100.0	40.6	32.5	SL
		95.3	36.3	23.6	SL
		92.8	23.6	15.7	SL
		88.5	14.1	8.9	SL
		85.6	6.8	3.5	SL
		83.5	2.1	−1.5	SL
		81.8	1.7	−5.6	SL
		78	3.4	1.3	SL
		75.1	26.7	25.8	LL
		73.5	34.6	34.3	LL
		70.4	47.1	46.4	LL
		68	56.5	55.6	LL
		63.7	66.5	66	LL
		60.9	72.8	72.5	LL
		58.2	77.6	77.6	LL
		56.2	80.6	80.3	LL
		53.9	81.3	81.3	LL
		51.8	82.5	82.4	LL
		49.6	83.5	83.5	LL
		45.3	83.8	83.6	LL
		41.2	87.5	87.5	LL
		36.1	89.6	89.4	LL
		31	90.4	90.2	LL
		27.1	91.6	91.3	LL
		24.6	91.6	91.6	LL
		22.2	90.2	89.8	LL
		20.0	90.5	90.1	LL
		18	91	90.6	LL
		16.5	89.2	88.8	LL
		15	86.7	86.7	LL
		13.6	83.3	83.3	LL
		12.5	80.6	80.5	LL
		11.2	76.5	76.5	LL
		10.3	71.9	71.8	LL
		9.7	69	69	LL
		8.9	64	63.7	LL
		8.1	59.8	59.3	LL
		7.2	51.6	51.4	LL
		6.6	46	45.9	LL
	90:10	100.0	33.7	28.2	SL
		94.5	19.4	17.1	SL
		90.5	11	8.7	SL
		85.3	2.8	0.6	SL
		80.3	−5	−8.8	SL
		78.5	−4	−6.4	SL
		75.7	−2.1	−5	SL
		70.0	−1.7	−3.6	SL
		64.2	30.3	28.9	SL
		54.4	52.5	52.1	LL
		49.6	65.3	64.7	LL
		44.6	72.6	71.8	LL
		39.9	76.5	76.4	LL
		35.1	79.1	78.9	LL
		29.9	81.4	80.0	LL
		24.9	81.1	79.7	LL
		20.0	78.3	77.1	LL
		15.2	71.3	70.8	LL
		10.3	55.8	54.9	LL
	80:20	100.0	49.8	21.1	SL
		91.4	26.8	−0.1	SL
		77.3	6	−11.7	SL
		65.6	1.3	−6.3	SL
		57	30.3	28.8	SL
		49.4	50.1	49.6	LL
		42.9	53.9	53.9	LL
		37.6	64.9	64.6	LL
		32.2	66.3	65.6	LL
		27.5	65.7	65.1	LL
		23.9	63.6	63	LL
		20.6	60.7	60.0	LL

Table 1. (*Continued*)

Solvent Composition (Water:Acetone)	Solute Ratio (Phenol:Catechol)	Experimental Data			
		Weight % Solute	Disappearance Temperature (°C)	Reappearance Temperature (°C)	Indication*
		18.9	57.2	57.1	LL
		16.7	53.8	53.6	LL
		14.8	48.8	47.8	LL
		12.8	42.5	42.3	LL
50:50	100:0 (pure phenol)	100.0	40.9	34.5	SL
		92.1	38.9	25.7	SL
		86.8	13.9	6.8	SL
		81.2	4.6	−10.1	SL
		75.8	−6.2	−12.8	SL
		68.1	1.1	−4.9	SL
		61.8	27.5	27.3	LL
		55.6	49	48	LL
		49.3	57.2	56.5	LL
		42.1	67.2	65.3	LL
		35.9	67.7	66.7	LL
		30.8	62.8	61.1	LL
		26.1	54.2	53.8	LL
		21.8	38	38.2	LL
		18.8	18.7	18.2	LL
	90:10	100.0	33.6	29.8	SL
		94.9	21.8	21	SL
		89.6	10.2	8.9	SL
		83.9	−1.5	−2.8	SL
		79.3	−9.9	−11.7	SL
		74.1	−4.9	−5.7	SL
		68.5	−1.8	−2.3	SL
		63.6	19.5	19.4	LL
		58.7	30.6	29.5	LL
		53.7	40.5	39.8	LL
		48.6	44.7	45.1	LL
		43.6	51.9	52.2	LL
		38.6	57.3	57	LL
		33.8	57.5	57.5	LL
		29	51.6	51.6	LL
		24.2	38.2	38.1	LL
		19.4	13	13	LL
		14.5	−10.8	−12	SL
		9.7	−13.2	−14.6	SL
	80:20	99.9	44.8	24.6	SL
		95.5	17.8	8.1	SL
		90.4	12.3	2	SL
		85	−4.3	−8.1	SL
		77.7	−14.1	−19.5	SL
		69.4	−10.1	−25.3	SL
		61.1	−6.8	−7.7	LL
		52.5	15.2	14.6	LL
		44.6	31.9	30.8	LL
		38.6	33	31.9	LL
		33.1	25.3	25.3	LL
		28	10.6	9.8	LL
	50:50	100.0	69.3	60.5	SL
		94.8	54.8	42.7	SL
		87.1	38.2	21.5	SL
		78.4	18.3	0	SL
		62.1	3.3	−14	SL
		54.8	−3	−13.9	SL
		41.7	−3.3	−13.1	SL
		33.9	−6.4	−10.7	SL
		28.9	−6.8	−13.7	SL
		23.6	−8.6	−13.4	SL
0:100 (pure acetone)	100:0 (pure phenol)	100.0	40.2	36	SL
		91.2	38.5	18	SL
		81	25.3	5.3	SL
		73.3	14.7	−0.2	SL
		66.5	11.6	−8.4	SL
		54.3	1.8	−15.2	SL
		49.2	−6.8	−20.7	SL
	90:10	100.0	34.3	29.6	SL
		94.1	26.1	22.8	SL
		88.7	15	12.5	SL

Table 1. (*Continued*)

Solvent Composition (Water:Acetone)	Solute Ratio (Phenol:Catechol)	Experimental Data			
		Weight % Solute	Disappearance Temperature (°C)	Reappearance Temperature (°C)	Indication*
		83.7	0.4	−2.1	SL
		79.1	15.8	−13.7	SL
		73.6	13.1	−17.8	SL
		68.6	10.5	−20.2	SL
		64	6.8	−25.7	SL
		59	2.8	−2.6	SL
		54.2	1.8	−7.8	SL
		49.6	−7.5	−23.7	SL
		44.6	−14.3	−17.2	SL
		39.6	−21.2	−25	SL
		34.9	−27.9	−56.7	SL
		29.4	−34.8	−49.6	SL
		24.7	−43.6	−58.3	SL
	80:20	100.0	52	24.6	SL
		95.4	35.2	16	SL
		90.6	27.3	9.3	SL
		86.2	22.9	−2.7	SL
		81.7	18.6	−5.4	SL
		77.7	14.3	−13.3	SL
		74.1	12.1	−13.7	SL
		70.7	10.6	−14.5	SL
		65.6	7	−18.6	SL
		60.5	1.7	−25.3	SL
		55.7	−3.7	−26.1	SL

*SL, solid–liquid boundary; LL, liquid–liquid boundary

confirms the validity of the suggested method for determining the SLLE phase diagram. Note that the overall trend also agrees with a typical SLLE phase behavior consisting of a liquid–liquid phase split region with a UCST (observed to be about 66°C for this binary system) sitting on top of an SLE region. The reversal of trend (the dissolution temperature decreases with increasing phenol content below 75 wt % but increases with increasing phenol content above 75 wt %) confirms the different nature of the phase boundaries: LLE on one side and SLE on the other. There is also a eutectic at about 7 wt % phenol, marked by a similar trend reversal but with SLE boundaries on both sides.

Figure 7b shows the experimental results for catechol/water binary system. Over the entire range of composition studied (16–90 wt % catechol), a relatively large difference between disappearance and reappearance temperatures is evident, indicating an SLE boundary without the presence of liquid–liquid phase split. The overall trend is consistent with the physical properties of catechol found in its Material Safety Data Sheet (melting point = 105°C and solubility in water at 20°C = 43 g/100 mL), which are plotted as open triangles in the figure. It is reasonable to assume simple eutectic behavior of this binary system, which implies that there is a eutectic below 16 wt % catechol. Since the objective of this experiment is to locate the liquid–liquid phase split region, no attempt was made to determine the exact location of that eutectic point.

Data for different cuts at constant phenol to catechol ratios, which form the interior of the 3D diagram, are also taken. Figures 7c, d depict pseudo-binary systems with a phenol to catechol ratio of 95:5 and 90:10 (by weight), respectively. A similar trend to phenol/water binary system (Figure 7a) can be observed, with the data on the catechol and phenol-rich side (above 70 wt % catechol + phenol) indicating the presence of an SLE boundary, while an LLE boundary is evident in the catechol + phenol concentration range of 10–60 wt %.

The trend is less clear for the pseudo-binary system with a phenol to catechol ratio of 80:20 (by weight) (Figure 7e). LLE boundary is evident in the catechol + phenol concentration range of 10–45 wt %, while the rest of the data seems to indicate an SLE boundary. Determination of solid identity was not attempted in this experiment, but it can bez speculated that the SLE boundary actually consists of two segments. Since the disappearance temperature of the 100 wt % catechol + phenol mixture is above the melting point of phenol of 40°C, the SLE boundary on this side of the phase diagram must represent liquid compositions that are in equilibrium with solid catechol. Meanwhile, as the LLE region appears in the binary phase diagram of phenol/water (Figure 7a) but not in that of catechol/water (Figure 7b), it is likely that the SLE boundary near the LLE region represents liquid compositions that are in equilibrium with solid phenol. This implies the existence of a double saturation point at which phenol and catechol are both saturated in water, possibly somewhere around 70–80 wt % of (catechol + phenol).

Figures 7f, g show two other pseudo-binary systems with a phenol to catechol ratio of 50:50 and 20:80 (by weight), respectively. Only SLE boundaries are observed in both systems, as evident by the significant difference between disappearance and reappearance temperatures. Apparently, the LLE region emanating from the phenol/water side of the triangular prism does not extend very far into the interior.

Next, pseudoternary systems of phenol/catechol/solvent with two different mixtures of water/acetone (water:acetone = 75:25 and 50:50 by weight) as the solvent were studied. Data for the ternary system phenol/catechol/acetone were also obtained to complete the picture. The experimental results for the three solvents are summarized in Table 1.

Isothermal cuts

Based on the disappearance temperature data, different isothermal cuts of the phenol/catechol/solvent phase diagram can be generated and plotted together to form a contour map. Figure 8a is the contour map for the ternary system phenol/catechol/water, showing isothermal cuts at seven different temperatures ranging from 20 to 80°C. The phase boundaries are obtained from the data shown in Figures 7a–g. The rectangles represent LLE boundary data, while the triangles correspond to compositions lying on an SLE boundary. The contour lines are drawn passing the data points in a manner consistent with the topology of the phase diagram. For example, at 20°C there are two SLE data points, lying on the phenol/water edge and on the cut at phenol:catechol = 95:5, respectively, which represent liquid compositions in equilibrium with solid phenol, while the rest of SLE data points at that temperature correspond to liquid compositions in equilibrium with solid catechol. Consequently, the contour line at 20°C is drawn in two segments, corresponding to the solubility curves of phenol and catechol, respectively. The two segments intersect at a double saturation point. A similar situation is observed at 30 and 40°C, except that at these temperatures the two segments do not intersect with each other and there is no double saturation point. No attempt was made to collect additional data since the SLE regions on the diagram are not the main targets of this experiment.

Figure 8b is the contour map for the pseudoternary system of phenol/catechol/solvent with water:acetone in the solvent = 75:25, which is constructed from three sets of data (cuts at phenol:catechol ratio of 100:0, 90:10, and 80:20 by weight). Similar to the case of pure water as the solvent (Figure 8a), the map features an LLE region near the phenol/solvent edge, and an SLE region close to the catechol vertex. LLE boundaries are still observed in the isothermal cuts at 70 and 80°C, and compared to the pure water case, the LLE boundaries at lower temperatures extend deeper into the interior of the triangle. Both of these are indications that the LLE region for this solvent is bigger than that for pure water. It can also be seen that the SLE region also appears to be bigger for this solvent compared to that for pure water, although

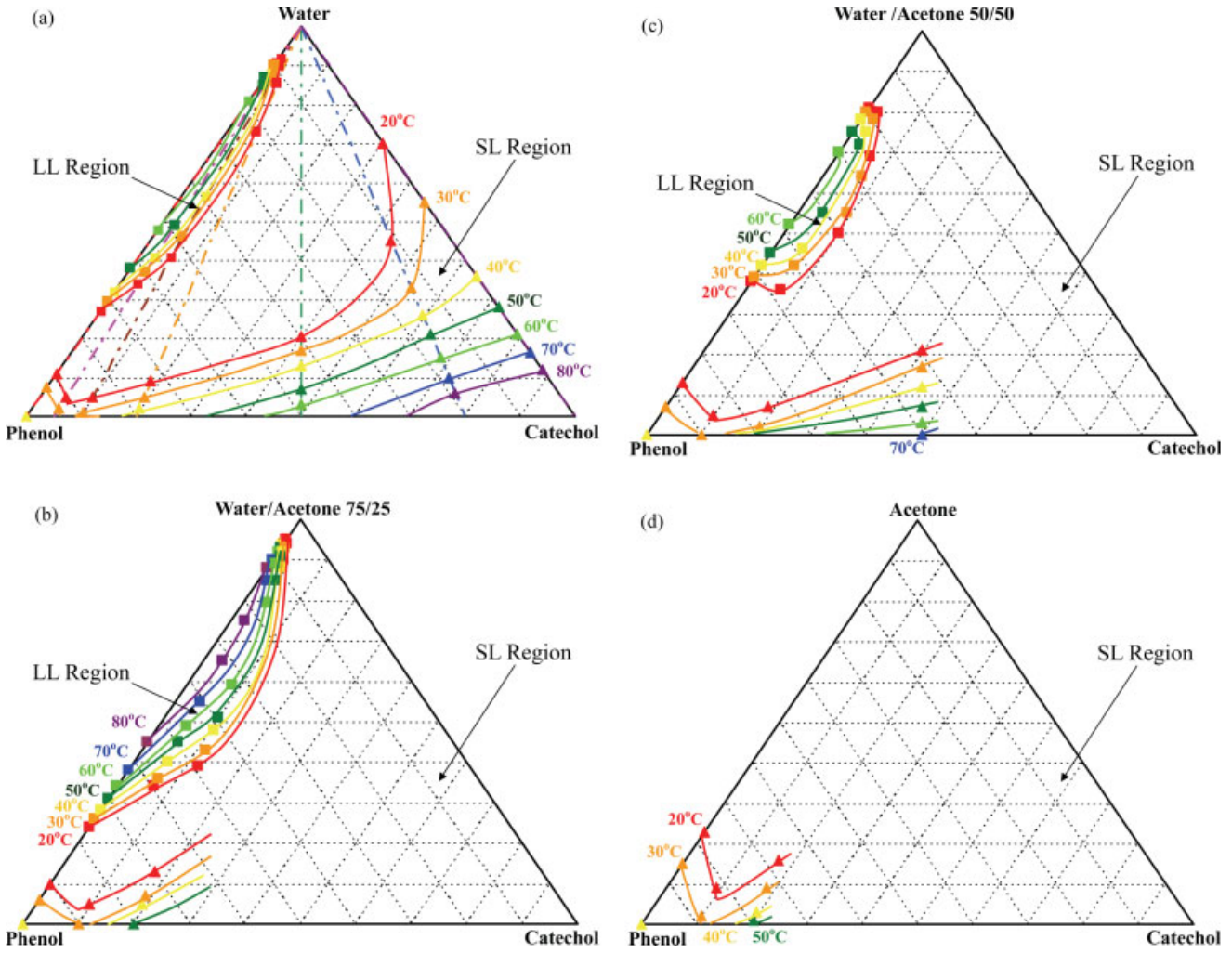

Figure 8. Isothermal plots of the phenol/catechol/solvent mixtures at different temperatures: (a) pure water, (b) 75/25 wt % water/acetone, (c) 50/50 wt % water/acetone, (d) pure acetone.

[Color figure can be viewed in the online issue, which is available at www.interscience.wiley.com.]

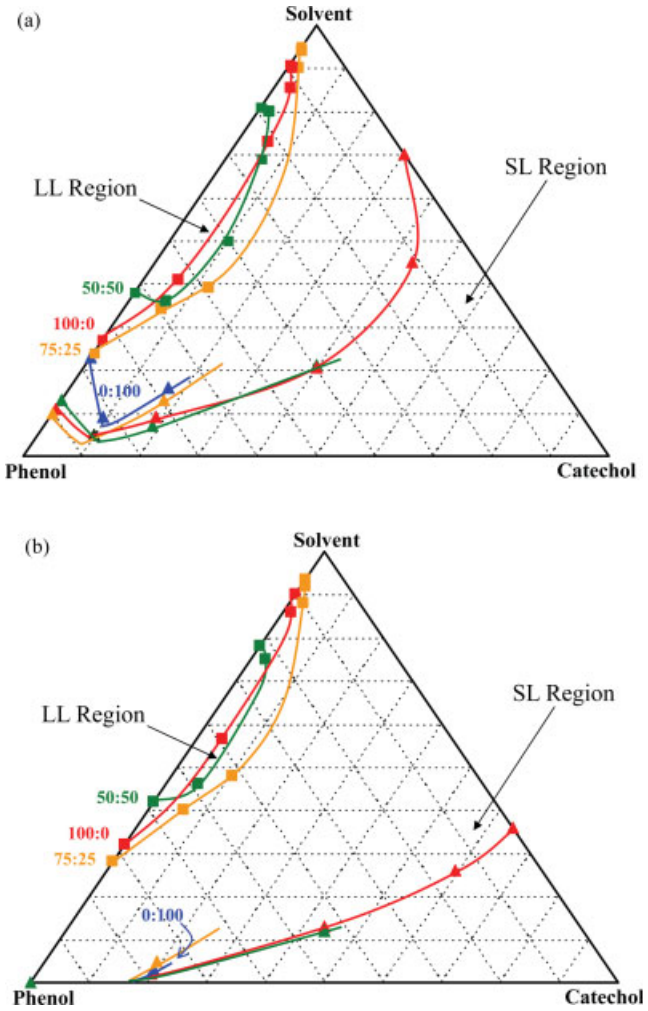

Figure 9. Isothermal cuts of the pseudo-ternary phenol/catechol/solvent systems for different solvent compositions: (a) at 20°C, (b) at 40°C.

[Color figure can be viewed in the online issue, which is available at www.interscience.wiley.com.]

no effort was made to determine the SLE boundaries and double saturation points for higher phenol to catechol ratios.

When the content of acetone in the solvent is increased to 50 wt %, the LLE region becomes smaller as can be seen from the contour map in Figure 8c, which is constructed from four sets of data (cuts at phenol to catechol ratio of 100:0, 90:10, 80:20, and 50:50). Similar to the case of pure water and water/acetone mixture with water to acetone ratio of 75:25, the size of the LLE region monotonically decreases as the temperature increases. No LLE boundary can be observed above 60°C for this solvent. Again, complete determination of the SLE region was not attempted.

A very different contour map is obtained if pure acetone is used as a solvent (Figure 8d). Since the highest disappearance temperature among all data used in this figure (cuts at phenol to catechol ratio of 100:0, 90:10, and 80:20) is 52°C, no isothermal cut above this temperature can be identified in the contour map. Furthermore, because all data have been identified as SLE boundary, there is no LLE region in this map. For the purpose of comparison with Figures 8a–c, only isothermal cuts at 20–50°C are shown. While isothermal cuts at lower temperature can be deduced from the experimental data, such cuts feature only SLE regions and are not shown here as SLE determination is not our main focus. For the same reason, no further attempt was made to determine additional cuts at lower phenol to catechol ratios.

Effect of solvent

To compare the effect of different solvents, the isothermal cuts for different solvent mixtures at the same temperature are plotted in the same coordinates. Figure 9a shows the isothermal cuts at 20°C for four different ratios of water to acetone (by weight) in the solvent, namely 100:0 (pure water), 75:25, 50:50, and 0:100 (pure acetone). A narrow LLE region near the phenol/solvent edge exists when pure water is used as the solvent (red curve). At water to acetone ratio of 75:25 (orange curve), the size of the region is significantly enlarged. However, this region becomes smaller at water to acetone ratio of 50:50 (green curve) and does not exist when pure acetone is used as the solvent. The size of the SLE region also varies with solvent composition, but the small number of data points does not allow for trend observation.

The equilibrium boundaries for different solvent compositions are also compared at 40°C by plotting the corresponding isothermal cuts (Figure 9b). Similar to the observed trend at 20°C, the size of the LLE region at 40°C increases then decreases as acetone is added to the system. No LLE region is found when the solvent is pure acetone. No SLE boundary is found along the phenol/solvent edge except the one very close to the phenol edge, since 40°C is just below the melting point of pure phenol. All SLE boundaries shown in Figure 9b are essentially the solubility curves of catechol in a mixed solvent containing phenol, water, and acetone. These curves converge to one point on the phenol/catechol edge, which represents the solubility of catechol in phenol at 40°C.

Conclusions

SLLE phase diagrams are useful for mapping out regions of temperature and compositions that are feasible for crystallization by avoiding liquid–liquid regions which may present various operational problems. A systematic approach for the experimental determination of the SLLE phase diagram for a system containing more than two components has been developed. The dimensionality of the system is reduced by taking appropriate cuts. This is followed by observing the disappearance and reappearance of a second phase in the system using an easy-to-use polythermal experimental technique. Both liquid–liquid and solid–liquid phase boundaries are identified. Combining the information from various cuts, the overall phase behavior can be deduced. Such an approach is particularly useful for systems with mixed solvents, since the occurrence of liquid–liquid phase split often depends on the solvent composition. As demonstrated in the example, the size of the LLE region in cuts at different solvent compositions does not necessarily follow a monotonic trend.

In this study, visual observation of turbidity was used to determine the disappearance and reappearance temperatures. While the method described here is applicable regardless of the observation method, its accuracy can be improved if an instru-

ment such as a turbidity meter were used to detect the phase split. The solvent composition as well as its physical properties such as viscosity and solubility is expected to impact not only the size and location of the liquid–liquid region but also the nucleation and growth kinetics. In the synthesis of a crystallization process,[16] it is crucial that all these tradeoffs are elucidated and quantified. Efforts in these directions are underway.

Acknowledgments

We thank Dr Haruki Asatani of Mitsubishi Chemical Corporation for his valuable comments on this work. Research support of the Research Grants Council (Grant HKUST602704) is gratefully acknowledged.

Literature Cited

1. Kim S, Wei C, Kiang S. Crystallization process development of an active pharmaceutical ingredient and particle engineering via the use of ultrasonics and temperature cycling. *Org Proc Res Dev*. 2003;7:997–1001.
2. Broide ML, Tominc TM, Saxowsky MD. Using phase transitions to investigate the effect of salts on protein interactions. *Phy Rev E*. 1996;53:6325–6335.
3. Mendiratta AK. Purification of Bisphenol-A. *United States Patent* 4,529,823,1985.
4. Lafferrere L, Hoff C, Veesler S. Study of liquid–liquid demixing from drug solution. *J Cryst Growth*. 2004;269:550–557.
5. Lafferrere L, Hoff C, Veesler S. In situ monitoring of the impact of liquid-liquid phase separation on drug crystallization by seeding. *Cryst Growth Des*. 2004;4:1175–1180.
6. Shang M, Matsuyama H, Maki T, Teramoto M, Lloyd DR. Effect of crystallization and liquid–liquid phase separation on phase-separation kinetics in poly(ethylene-*co*-vinyl alcohol)/glycerol solution. *J Polym Sci Part B: Polym Phys*. 2003;41:194–201.
7. Bonnett PE, Carpenter KJ, Dawson S, Davey RJ. Solution crystallization via a submerged liquid–liquid phase boundary: oiling out. *Chem Commun*. 2003;6:698–699.
8. Kwok KS, Chan HC, Chan CK, Ng KM. Experimental determination of solid–liquid equilibrium phase diagrams for crystallization-based process synthesis. *Ind Eng Chem Res*. 2005;44:3788–3798.
9. Raal JD, Muhlbauer AL. Phase equilibrium measurement and computation. Washington, DC: Taylor & Francis, 1998, Chapter 3:97–103.
10. Harjo B, Ng KM, Wibowo C. Visualization of high-dimensional liquid–liquid equilibrium phase diagrams. *Ind Eng Chem Res*. 2004;43:3566–3576.
11. Ricci JE. Systems with two liquid phases. In: The Phase Rule and Heterogeneous Equilibrium. New York: Van Nostrand, 1951, Chapter VIII.
12. Hamamoto T, Umemura S. Phenol derivatives. In: Gerhartz W, Yamamoto Y S, Campbell FT, Pfefferkorn R, Rounsaville JF, editor. *Ullmann's Encyclopedia of Industrial Chemistry*. Weinheim, Federal Republic of Germany: VCH, Vol. A19, 1995:313.
13. Jacques B, Daniel C. Method and installation for separating and purifying diphenols in the phenol and phenol derivatives industry. United States Patent 6,844,472 B1, 2005.
14. Gajanan KD, Vinay VT, Sanjeevani AP, Arumugam S, Sukumar D. Process for conversion of phenol to hydroquinone and quinines. United States Patent 6,872,857 B1, 2005.
15. Campbell AN, Campbell AJR. Concentrations, total and partial vapor pressures, surface tensions and viscosities, in the systems phenol-water and phenol-water-4% succinic acid. *J Am Chem Soc*. 1937;59:2481–2488.
16. Wibowo C, Ng KM. Unified approach for synthesizing crystallization-based separation processes. *AIChE J*. 2000;46:1400–1421.

Manuscript received Aug. 7, 2006, revision received Oct. 29, 2006, and final revision received Mar. 22, 2007.